Peña Station NEXT Energy District Master Plan

Cooperative Research and Development Final Report

CRADA Number: CRD-17-681

NREL Technical Contact: Bri-Mathias Hodge

Authors: Kate Doubleday, Andrew Parker, Faeza Hafiz, Benjamin Irwin, Samuel Hancock, Shanti Pless, and Bri-Mathias Hodge

NREL is a national laboratory of the U.S. Department of Energy
Office of Energy Efficiency & Renewable Energy
Operated by the Alliance for Sustainable Energy, LLC

This report is available at no cost from the National Renewable Energy Laboratory (NREL) at www.nrel.gov/publications.

Contract No. DE-AC36-08GO28308

Technical Report
NREL/TP-5D00-76242
February 2020

Peña Station NEXT Energy District Master Plan

Cooperative Research and Development Final Report

CRADA Number: CRD-17-681

NREL Technical Contact: Bri-Mathias Hodge

Authors: Kate Doubleday, Andrew Parker, Faeza Hafiz, Benjamin Irwin, Samuel Hancock, Shanti Pless, and Bri-Mathias Hodge

Suggested Citation
Doubleday, Kate, Andrew Parker, Faeza Hafiz, Benjamin Irwin, Samuel Hancock, Shanti Pless, and Bri-Mathias Hodge. 2020. *Peña Station NEXT Energy District Master Plan: Cooperative Research and Development Final Report, CRADA Number CRD-17-681.* Golden, CO: National Renewable Energy Laboratory. NREL/TP-5D00-76242. https://www.nrel.gov/docs/fy20osti/76242.pdf.

NREL is a national laboratory of the U.S. Department of Energy
Office of Energy Efficiency & Renewable Energy
Operated by the Alliance for Sustainable Energy, LLC

This report is available at no cost from the National Renewable Energy Laboratory (NREL) at www.nrel.gov/publications.

Contract No. DE-AC36-08GO28308

Technical Report
NREL/TP-5D00-76242
February 2020

National Renewable Energy Laboratory
15013 Denver West Parkway
Golden, CO 80401
303-275-3000 • www.nrel.gov

Cooperative Research and Development Final Report

Report Date: 2/27/20

In accordance with requirements set forth in the terms of the CRADA agreement, this document is the final CRADA report, including a list of subject inventions, to be forwarded to the DOE Office of Science and Technical Information as part of the commitment to the public to demonstrate results of federally funded research.

Parties to the Agreement: Panasonic Enterprise Solutions Company ("Panasonic")

CRADA number: CRD-17-681

CRADA Title: Peña Station NEXT Energy District Master Plan

Joint Work Statement Funding Table showing DOE commitment:

Estimated Costs	NREL Shared Resources a/k/a Government In-Kind
Year 1	$250,000.00
TOTALS	$250,000.00

Abstract of CRADA Work:

The objective of the project is to work in close collaboration with Panasonic, Xcel Energy (Public Service), and their partners L.C. Fulenwider, and Denver International Airport to examine different design and technology options in creating an energy master plan for the 400 acre Peña Station NEXT district in Denver, Colorado. To accomplish this, NREL will conduct a solar power/battery storage/grid integration study using the OpenDSS platform linked to UrbanOPT software.

Summary of Research Results:

RISING global interest in greenhouse gas reductions and energy conservation is spurring the development of sustainable communities and smart cities [1]. The culmination of this trend is the net zero energy (NZE) district or town, which on average produces enough energy on-site to offset its consumption, typically balanced over an annual time horizon [2], [3]. To achieve NZE, these communities generally employ high-efficiency building measures and distributed energy resources (DERs), such as solar photovoltaics (PV); however, the sustainable and NZE district planning process typically does not include consideration of the electric distribution system and assumes that the grid can accommodate any magnitude of power import or export at any time [4]. Even when a finer hourly or subhourly time resolution is considered, the distribution system is often excluded or much simplified [5], [6]. Neglecting grid impacts from high DER penetrations during the design phase can result in a variety of complications, including power backfeeding, voltage violations, and inappropriate protective equipment responses. As a result,

the district developer might be faced with costly infrastructure reinforcements or unanticipated DER curtailment that interferes with the district's ability to achieve NZE in practice [7].

Centralized planning of a district's buildings and distribution system, including its DERs and their operational impacts, could mitigate these challenges and improve NZE performance (Task 1). Integrating building and distribution system models in one framework enables developers and system operators to compare investment in demand-side technologies (e.g., energy efficiency, demand response) with supply-side technologies (e.g., renewable DERs, electrical energy storage systems (ESS), smart inverters) to determine possible system architectures; however, advances in data-driven modeling and new control schemes are required from the research community to enable highly detailed integrated district planning, especially when improving the design process to consider operations. Most district design processes have excluded detailed distribution system models, but recent modeling frameworks have started to address this gap. Morvaj et al. [8] presents a planning and operations optimization tool incorporating building simulations in EnergyPlus with distribution grid models. Another such framework is MESCOS, which interfaces commercial software to model building loads; system controls; and gas, heat, and electricity networks [9]. In [10], PV generation and building loads are modeled endogenously based on occupant activity data. The IDEAS library also models building activities and loads, thermal systems, DERs, the distribution grid, and various controls endogenously [7], [11]. These previous works have applied their integrated frameworks to primarily study grid impacts of distributed PV combined with demandside management or district heating networks.

As one contribution of this work, we take a new perspective of applying integrated building and power system modeling to the task of designing a NZE electrical system, assuming utility ownership and operation of DERs through rate-based investments [12]. In these modeling frameworks, electrical energy storage has not explicitly been included, but it is key for achieving net zero import on any time resolution less than 1 day by time shifting energy from renewable DERs, particularly PV because it produces power only during daylight hours. This requires new control strategies for the coordinated control of district ESS with hourly or subhourly NZE performance in mind. For example, NZE goals are addressed in [13], which uses centralized ESS control to smooth a community's net load. More frequently, ESS control within distribution systems has been treated as a profit maximization problem for third-party owners or as a cost and power quality optimization from a utility perspective [14]–[16]. Extensive work has also been done on ESS operations in islandable microgrids [17], which extend the NZE idea to complete self-sufficiency; however, most districts occupy the middle ground where islanding is unnecessary and simpler heuristic control methods are valuable to enable NZE design without prohibitive computation.

Additionally, a utility-operated NZE district should proactively address operational challenges, including voltage rise from DERs. Besides classic mechanisms such as load tap changers (LTCs), inverter-interfaced DERs can mitigate voltage rise through reactive power absorption and active power curtailment. A variety of control approaches have been proposed [18], ranging from central or decentralized optimizations [15], [19], [20] to local control heuristics, which cannot guarantee global optimum but are easy to implement. Among these, linear piecewise volt/var (VVAR) and volt/watt (VW) droop control will likely receive practical implementation because of the adoption of the newest version of IEEE 1547 [21]. Current research is addressing the selection of droop parameters as well as combined VW/VVAR approaches [22]–[24].

The contributions of this work include a novel district control scheme with modified VW/VVAR control for modeling districts aiming to achieve subhourly NZE while mitigating potential grid impacts. This includes a coordinated ESS control scheme that accounts for network losses, storage losses, and available storage capacity. We also develop a highly detailed integrated modeling platform with open-source building and distribution system models to simulate a district's performance at 15-minute resolution for 1 year (35,040 time steps). As a case study, the modeling platform is applied to design of Peña Station NEXT, a new 100-building, 400-acre district on a 1,200-node distribution feeder using actual utility, developer, and weather data from 2016. To focus on the design of the district's DERs, the integrated framework is applied in an exhaustive analysis of the DER design space through 2,551 scenarios to inform the decision process by comparing the scenarios' affordability, self-sufficiency, and grid reliability.

NZE District Objectives

A NZE district must serve the needs of multiple stakeholders, including its residents and customers, the district developer, and the local utility (Task 1). In this work, we apply a multiobjective design process to balance these competing needs by considering the self-sufficiency, investment cost, and reliability of the power system. In the following formulation, B denotes the set of in-district building and block locations where loads and DER assets are located, and subscript i indexes a particular location in B. $P_{load,i}(t)$, $P_{PV,i}(t)$, and $P_{ESS,i}(t)$, are the building load, PV, and ESS powers (kW), respectively, at location i at time step t; $P_{load}(t)$, $P_{PV}(t)$, and $P_{ESS}(t)$ (positive for discharging) are the in-district coincident sums.

The NZE metrics proposed here quantify a district's electrical self-sufficiency and sustainability if using renewable DERs. Although multiple NZE definitions are available [3], they typically consider a region that can generate as much energy as it consumes over some time horizon to be NZE; however, this obscures losses within the distribution system, renewable curtailment, and other power system impacts important to the utility. Therefore, we define a NZE electrical system as a geographically contiguous portion of a power grid that exports as much electrical energy as it imports during a balancing period. NZE communities commonly consider a balancing period of one year, so the annual net energy import (ANEI) is defined as the sum of the district import energy during the year, where T is the period between time steps (0.25 h) and $P_{im}(t)$ (kW) is the district import power, which can be negative: $\text{ANEI (kWh)} = \sum_t T \times P_{im}(t)$.

Although ANEI is useful in broad strokes, it assumes that the grid can always accommodate the district's power imbalance, obscuring challenges such as backfeeding. Achieving NZE at a finer hourly or subhourly timescale can minimize detrimental impacts, particularly to the utility. The cumulative power imbalance (CPI) sums the magnitude of the district power imbalance during the year to measure subhourly NZE: $\text{CPI (kW)} = \sum_t |P_{im}(t)|$. A district that is balanced at every time point will have zero CPI. By considering both annual and sub hourly balancing, implications of the two approaches can be compared.

Next, the DER and transformer investment cost for a particular scenario is considered. The DERs in this study are PV and ESS, but other district assets can be included. Commercial PV investment costs, $C_{PV,kW}$ ($/kWdc), include the cost of panels, inverters, and overhead and balance-of-system costs. Distributed ESS are modeled here as Lithium-ion batteries, with costs

broken into the battery cost, $C_{ESS,kWh}$ ($/kWh), and the balance-of-system cost, $C_{ESS,kW}$ ($/kW). Therefore, the utility's total investment cost is calculated as:

$$C = C_{PV,kW} \times \sum_{i \in B} P_{PV,DC,i} + \sum_{i \in B} C_T(S_{T,i}, X) + C_{ESS,kWh} \times \sum_{i \in B} E_i + C_{ESS,kW} \times \sum_{i \in B} S_{ESS,i}$$

where $P_{PV,DC,i}$ (kWdc) is the PV rating under standard test conditions; $S_{T,i}$ (kVA) is the transformer rating; C_T is a lookup function of transformer costs from X, the utility's catalog of options; and E_i (kWh) and $S_{ESS,i}$ (kVA) are the ESS energy capacity and inverter rating.
Last, system performance is assessed by the annual sum of line ampacity and node under- and overvoltage violations:

$$V = \sum_{t} \left(V_{amp}(t) + V_{UV}(t) + V_{OV}(t) \right)$$

where $V_{amp}(t)$ is the number of feeder lines violating their ampacity limits, $V_{OV}(t)$ is the number of feeder nodes violating the ANSI overvoltage limit (1.05 p.u.), and $V_{UV}(t)$ is the number of nodes violating the undervoltage limit (0.95 p.u.).

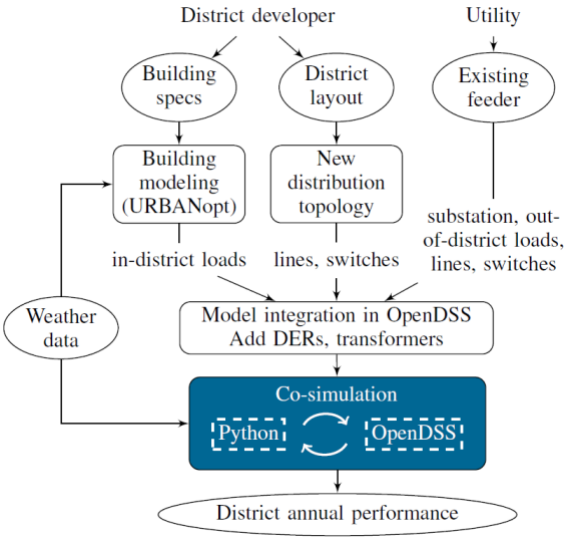

Figure 1. Block diagram of integrated district simulation framework, including buildings modeling in URBANopt leading into Python/OpenDSS distribution system cosimulation.

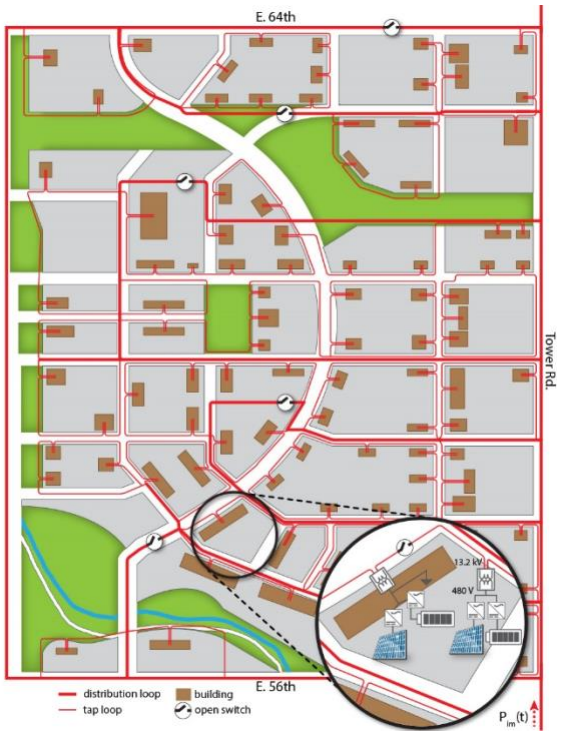

Figure 2. Peña Station NEXT, including its import power, $P_{im}(t)$, and block, building, and distribution line layout. The inset details one block's building loads, DERs, 13.2-kV-to-480-V transformers, and tap loop open point.

Together, these objectives can be used to compare district scenarios to ensure that the district developer can achieve its self-sufficiency goals, the utility can operate the system reliably, and the costs passed down to customers are affordable.

Integrated Load and Generation Modeling

To assess these multiple objectives for different district scenarios, a simulation framework integrating open-source tools is developed to endogenously model buildings, DERs, and the distribution system (Task 2). Figure 1 shows the simulation block diagram, and Figure 2 illustrates the model components for the Peña Station NEXT case study. First, the individual buildings within the district are modeled in URBANopt [25], a district-level modeling tool developed around OpenStudio [26]. Inputs are received from the district developer for each building's square footage, height, and use type (Task 3). A variety of demand-side technologies can be incorporated into URBANopt, such as higher insulation, all-LED lighting, or advanced ventilation systems. Based on the developer inputs, technology selection, and local weather data, each building's electrical load is simulated at 15-minute resolution over one year (Task 4). These electrical loads are exported into OpenDSS, an open-source power flow solver for distribution systems [27] (Task 5). For future work, the power system state can be fed back into URBANopt for coordinated building and power system controls, including demand response with thermal comfort constraints.

To incorporate DERs into the model, rooftop PV is added to each building and car canopy or ground-mounted PV to each city block; ESS are connected at each of these locations as well

(Figure 2 inset). A PV system's time-varying inverter output is modeled endogenously in OpenDSS based on the same weather data used in the building models, according to:

$$P_{PV,i}(t) = \min\left\{P_{PV,DC,i}\frac{I(t)}{1kW/m^2}\eta_{inv}\eta_{PV}(T_{PV}), S_{PV,i}\right\}$$

$S_{PV,i}$ is the inverter rating, η_{inv} is the constant inverter efficiency, and $I(t)$ (kW/m2) is the irradiance. $\eta_{PV}(T_{PV})$ is the temperature-dependent efficiency estimated for a typical Sunpower module, and $T_{PV}(t)$ is the weather-dependent module temperature simulated in SAM [28] for a typical fixed roof-mounted commercial system with 20° tilt. ESS operation during the course of the year is addressed in the section on battery modeling below. Determining the appropriate capacity of PV and ESS installations to balance the trade-off between investment costs and district self-sufficiency is one of the major design questions at hand, addressed in the case study section below.

Next, medium-voltage (13.2-kV) distribution lines are modeled from the new district assets to interconnect with the existing distribution feeder. Based on the layout determined by the district developer, new distribution lines are delineated according to utility practice (Figure 2). “Tap loops” connect the transformers around each block with low-ampacity lines. The tap loop connects to the load, PV, and ESS at each building or block site through a 13.2-kV-to-480-V three-phase transformer selected from the utility's catalog to ensure that its kVA rating minimally exceeds the maximum of the building peak load and the sum of the PV and ESS inverter ratings. High-ampacity “distribution loops” connect multiple tap loops back to the existing distribution feeder. Line impedances and ampacities are provided by the utility's proprietary hardware catalog. As indicated in the detailed figure inset, each of these physical loops contains an open switch, and it is not operated as an electrical loop. As with the building models, the distribution topology is exported into OpenDSS.

At the final stages of integration, these components are synthesized into one model in OpenDSS. In addition to the district components, the existing feeder and its loads are added to the model, allowing for holistic simulation of district interactions with surrounding neighborhoods and impacts at the substation level. Based on utility data, the existing feeder is modeled with time-synchronous power data from the same year as the weather data used in the district load and PV models. To simulate the district operation at subhourly resolution during one year, the OpenDSS model is cosimulated with customized controls implemented in Python, detailed next (Task 7).

District Control Algorithm:

Within the modeling framework, a new control algorithm is required to model the particular behavior of a NZE district. To pursue NZE on a subhourly basis, a centralized, coordinated control scheme for district DERs is developed. It is assumed that perfect load and PV forecasts are available; battery state of charge (SOC) can be accurately estimated; DERs are operated by the utility; and a supervisory control and data acquisition (SCADA) system monitors the distribution lines entering the district and communicates with local controllers at each building and block interconnection. Given the multiobjective focus, a heuristic control algorithm is developed to balance the NZE objective with grid stability requirements. The control scheme is intended to emulate the desired behavior for a wide range of scenarios; once likely district designs are selected, further operational optimizations can refine performance.

The control scheme, implemented for each time point in the annual simulation, is illustrated in Figure 3. An initial power flow is run in OpenDSS to select the substation LTC position to maintain 1.05 p.u. voltage on its secondary side. ESS powers are iteratively resolved to smooth the district's net load and achieve zero power import, if possible. PV VW/VVAR control is converged to minimize remaining overvoltage issues. The control scheme is implemented in Python, with the impacts of each decision assessed by rerunning the OpenDSS power flow. ESS and PV control phases are detailed below.

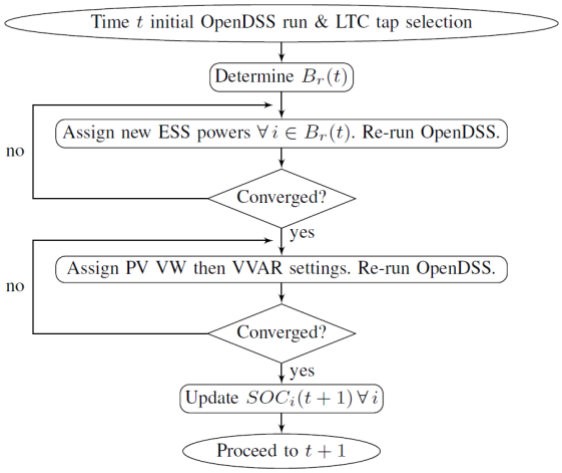

Figure 3. Control scheme of in-district DER assets at each time-point.

ESS Energy Time-Shifting

For a NZE district with only PV generation, the primary objective of ESS is to time-shift PV energy from day to night to even out the district's load throughout time, ideally achieving zero CPI; however, undesirable behavior occurs if the controller simply tries to minimize the district power import at each time point regardless of current ESS SOC and future conditions. For instance, in Figure 4, ESS charge with excess PV power until reaching maximum SOC, causing a large spike in uncurtailed power exported from the district. Achieving zero power import in the short-term results in more erratic behavior, increased reverse power flows, and increased likelihood of ampacity and voltage violations in the long term.

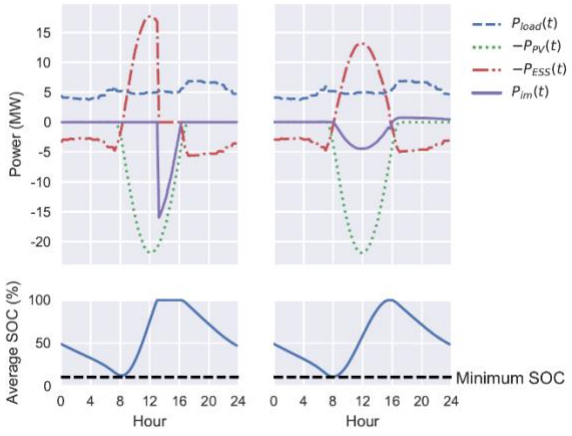

Figure 4. Impact of ESS control strategy on district power import without (left) and with (right) a forecasted look-ahead.

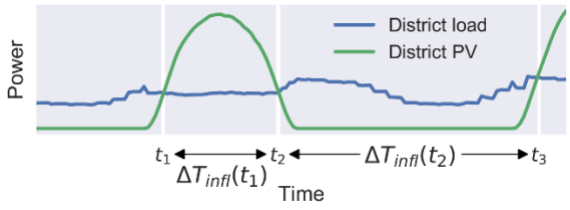

Figure 5. Inflection time points are identified to help smooth ESS (dis)charging behavior, given the anticipated load and generation imbalance during the time interval to the next inflection point.

This behavior is improved by using load and PV forecasts, from which inflection points can be determined, as shown in Figure 5. When district load rises above PV generation (and vice versa), ESS should switch from charging to discharging (and vice versa) to achieve the ideal zero power import; however, ESS might not have sufficient energy to supply district load until the next inflection point (or sufficient headroom to charge all excess PV power). Therefore, a look-ahead damping factor, $\lambda(t)$, is calculated at each inflection point to smooth (dis)charging behavior until the next inflection. ESS charging is slowed to a fraction of the ideal power with the goal of reaching the SOC limit just at the next inflection point. As demonstrated in Figure 4, this approach smooths ESS behavior by sacrificing some zero import performance in the short-term to mitigate undesirable grid impacts. Given this trade-off, a goal of the multiobjective scenario analysis is to determine adequate DER capacities to minimize the impact of the look-ahead and maintain zero import as much as possible.

This ESS control algorithm is executed as follows. The forecasted energy imbalance during the time interval $\Delta T_{infl}(t)$ from time t to the next inflection point is calculated from the equation for $P_{PV}(t)$ above and the building load profiles as:

$$E_{im}(t) = \left| \sum_{\tau=t}^{t+\Delta T_{infl}(t)} \left(P_{PV}(\tau) - P_{load}(\tau)\right) \right|$$

The upward and downward ESS energy capacities, accounting for losses and SOC limits, are calculated, respectively, as:

$$E_{up}(t) = \sum_{i \in B} \sqrt{\eta_{RT}} E_i \frac{(\overline{SOC} - SOC_i(t))}{100}$$

$$E_{down}(t) = \sum_{i \in B} \sqrt{\eta_{RT}} E_i \frac{(SOC_i(t) - \underline{SOC})}{100}$$

η_{RT} is the ESS round-trip efficiency, and $\overline{SOC}$ and $\underline{SOC}$ are the maximum and minimum allowable SOC, respectively. If it is an inflection point, a new look-ahead damping factor is calculated from these equations; otherwise, it remains the same:

$$\lambda(t) = \begin{cases} \min\left\{\frac{E_{up}(t)}{\rho E_{im}(t)}, 1\right\}, & \text{if } P_{load}(t-1) \geq P_{PV}(t-1) \text{ and } P_{load}(t) < P_{PV}(t) \\ \min\left\{\frac{E_{up}(t)}{\rho E_{im}(t)}, 1\right\}, & \text{if } P_{PV}(t-1) \geq P_{load}(t-1) \text{ and } P_{PV}(t) < P_{load}(t) \\ \lambda(t-1) & \text{otherwise} \end{cases}$$

An optional uncertainty factor, ρ, can be added as a conservative measure to account for both forecasting errors and distribution system losses that are not included in $E_{im}(t)$.

Next, an initial OpenDSS power flow is run with all PV systems generating at their maximum power points to determine the district power import. Given current ESS SOCs, only some systems might be able to (dis)charge as needed to reduce the power import to zero. The responsive subset is defined as:

$$B_{res}(t) = \begin{cases} \{i \in B | SOC_i(t) > \underline{SOC}\}, & P_{im}(t) \geq 0 \\ \{i \in B | SOC_i(t) < \overline{SOC}\} & \text{otherwise} \end{cases}$$

Next, the central controller enters an iterative loop to adjust the responsive ESS (dis)charge powers until convergence is reached. Iterative convergence is required because the ESS power needed to achieve zero instantaneous import does not equal the difference of load and generation because of distribution system losses. At each iteration j through the control loop at time t, the ideal new output power of each responsive ESS is calculated from its share of the previous district import power:

$$P_{new,i}(t,j) = P_{ESS,i}(t,j-1) + P_{im}(t,j)\frac{S_{ESS,i}}{\sum_{i \in B_{res}(t)} S_{ESS,i}}$$

Each responsive ESS is updated with the desired output power, constrained by its inverter rating:

$$P_{ESS,i}(t,j) = \lambda(t)\min\left\{\max\left\{-S_{ESS,i}, P_{new,i}(t,j)\right\}, S_{ESS,i}\right\} \forall i \in B_{res}(t)$$

The remaining ESS that do not have the SOC capacity to respond always have zero power (i.e., $P_{ESS,i}(t,j) = 0 \; \forall i \notin B_{res}(t) \; \forall j$). The OpenDSS simulation is then re-run to assess the impact of the new set points on the district power import.

Convergence may be reached in two ways: the power crossing the district boundaries is within a NZE tolerance, ε_Z, (i.e. $|P_{im}(t,j)| < \varepsilon_Z$), or the district import has reached a nonzero steady state because of the look-ahead damping factor or ESS power ratings, where change between iterations is within a small value, ε_C, (i.e. $|P_{im}(t,j) - P_{im}(t,j-1)| < \varepsilon_C$). Last, the SOC is updated according, constrained to ensure $\underline{SOC} \leq SOC_i(t+1) \leq \overline{SOC}$, where $SOC_i(1) = 50\% \; \forall i$:

$$SOC_i(t+1) = SOC_i(t) - \frac{\varphi P^*_{ESS,i}(t) T}{E_i} \times 100$$

Where: $\varphi = \begin{cases} \sqrt{\eta_{RT}}, & \text{if } P^*_{ESS,i}(t) < 0 \text{ (i.e., charging)} \\ \frac{1}{\sqrt{\eta_{RT}}}, & \text{otherwise} \end{cases}$

The asterisk indicates final values from the control loop.

Table 1
Voltage Droop Parameters

	P_a/Q_a	P_b/Q_b	$V_a\,(pu)$	$V_b\,(pu)$
VW	$P_{PV,i}(t,0)$	$max\{-P^*_{ESS,i}(t),0\}$	1.05	1.10
VVAR	0	$-\overline{Q_{PV,i}}(t,k)$	1.00	1.10

PV Voltage Control

Once ESS powers are selected, PV voltage control is added in a second iterative loop.

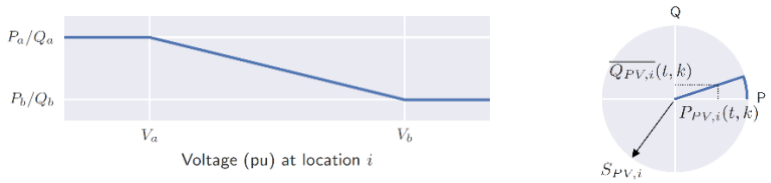

(a) (b)

Figure 6. (a) Piecewise linear VW\VVAR droop curve. (b) Maximum reactive power for VVAR is limited by power factor and inverter rating.

A controller at each PV/ESS pair monitors the local voltage, $V_i(t)$, and applies first VW and then VVAR control. Fig 6(a) illustrates the linear piecewise droop curve, and Table 1 reports the droop parameters, based on industry standards in [21]; however, to customize the VW control for a NZE district, PV generation is curtailed no further than the charging level of its ESS pair to avoid interference with the selected set points. Therefore, the VW equation for iteration k at time t if $V_{a,VW} \le V_i(t,k-1) \le V_{b,VW}$ is:

$$P_{PV,i}(t,k) = P_{PV,i}(t,0) - m_i(t)\left[V_i(t,k-1) - V_{a,VW}\right]$$

where $P_{PV,i}(t,0)$ is the uncurtailed power, and the slope is:

$$m_i(t) = \frac{P_{PV,i}(t,0) - \max\{0, -P^*_{ESS,i}(t)\}}{V_{b,VW} - V_{a,VW}}$$

Next, each smart inverter implements VVAR control as:

$$Q_{PV,i}(t,k) = -\overline{Q_{PV,i}}(t,k)\,\frac{V_i(t,k-1) - V_{a,VVAR}}{V_{b,VVAR} - V_{a,VVAR}}$$

if $V_{a,VVAR} < V_i(t,k-1) < V_{b,VVAR}$. The maximum allowable reactive power, $\overline{Q_{PV,i}}(t,k)$, is limited by a 0.97 power factor, as illustrated in Figure 6(b), to avoid excessive reactive power absorption in scenarios with high capacities of installed PV. This algorithm focuses on mitigating

overvoltages from DERs in close urban districts where voltage drops along the feeder are small but undervoltage VAR support can be similarly applied. The VW-VVAR logic is iterated until the average voltage change at the DER locations converges within a voltage tolerance, ε_V (i.e., $\frac{\sum_{i\in B}|V_i(t,k-1)-V_i(t,k)|}{|B|} < \varepsilon_Z$).

Application to Peña Station NEXT

The simulation framework is applied to design Peña Station NEXT (PSN), a developing 100-building, 400-acre mixed-use urban district in Denver, CO, for which solar is the only viable local renewable resource.

URBANopt Building Simulations

The new development comprises 6 low- and 39 high-density residential buildings, 3 hotels, 26 offices, 11 full and quick-service restaurants, and 8 stand-alone and 10 strip-mall stores. Based on the developer's specifications, the electrical load of each building is simulated in URBANopt at 15-minute resolution (i.e., $T = 0.25$ h) with 2016 weather data recorded near the development. Two efficiency scenarios are considered: a baseline compliant with ASHRAE 90.1-2013 building code [29] and a high-efficiency case, which includes reduced infiltration and plug load, increased insulation, all-LED lighting, increased effectiveness energy-recovery ventilators, and smart outdoor lighting controls (Tasks 4 & 5). The high efficiency case reduces annual electricity demand by 20% from 52.0 GWh to 41.5 GWh, with significant reduction of daily and annual peak loads, as shown in Figure 7. Given its significant impact on electric load, the multiobjective DER scenario analysis performed next is demonstrated with the high efficiency building scenario.

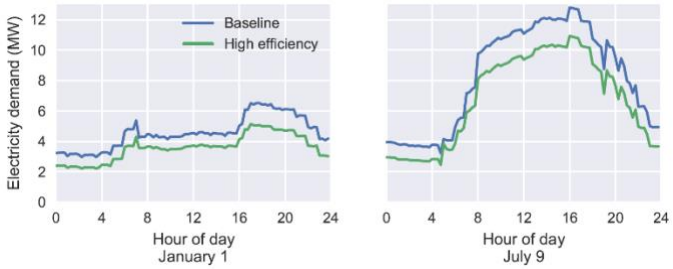

Figure 7. Total district electricity use is reduced by high efficiency measures, illustrated for (left) January 1 and (right) the peak load day, July 9.

Power System Description and DER Scenarios

The proposed distribution system serving PSN is illustrated in Figure 2 and interconnected with a proprietary model of the local distribution feeder extending to the nearest substation, provided by Xcel Energy. Out-of-district loads in the surrounding neighborhoods are modeled with a time-synchronous 2016 load profile measured at the feeder substation. The power system model including PSN comprises ~1,200 nodes.

For the high efficiency building scenario, a host of DER scenarios are considered to evaluate the multiple objectives explained above. To calculate investment costs, Li-ion battery costs from 2015 and turnkey PV costs from 2017 are used from [30] and [31], respectively. Although battery costs have dropped significantly in the last few years, this will change the magnitude but not the trends of the results. The maximum PV capacity at each building and city block is

geographically constrained by the rooftop and car canopy area. Fifty percent of the building area is allocated for rooftop PV with an industry typical fill factor of 18 W/ft2, assuming 20% efficient PV panels. Forty percent of the remaining area on the city blocks is allocated for car canopy and ground-mounted installations, with a fill factor of 0.2 MW/acre. The maximum ESS capacity at each location is proportional to its PV capacity, so the total allowable in-district energy capacity is 500 MWh. This capacity is selected to determine if the district can achieve 15-minute NZE during the period of lowest PV generation, a 3-day clouded period in winter during which the total in-district load is ~430 MWh.

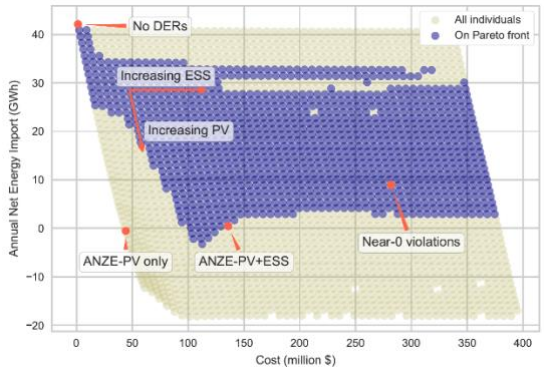

Figure 8. Annual NZE, indicated by zero ANEI, is reached with ~27 MW of installed PV. With higher PV installations, the district has net positive energy.

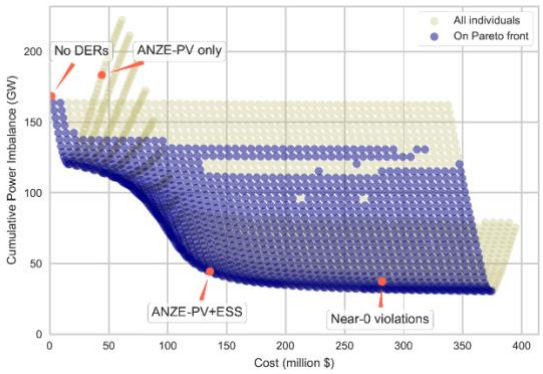

Figure 9. 15-minute NZE, corresponding to zero CPI, is not achieved for the DER scenarios considered here, but significant improvement can be made by adding battery storage for intraday energy time-shifting.

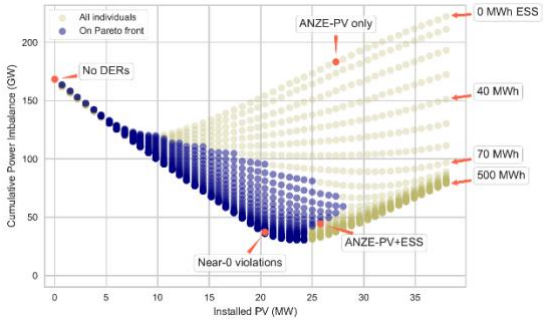

Figure 10. CPI decreases with increasing PV penetration, up to a point where curtailment and power backfeeding deteriorate performance.

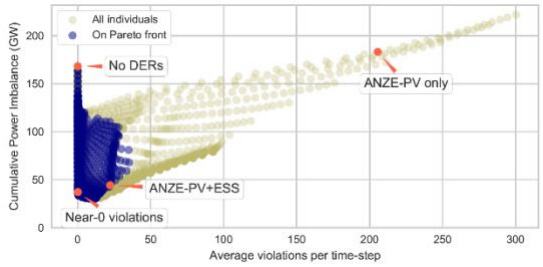

Figure 11. Average operational violations per time step, with voltage violations counted for the 1,173 nodes and ampacity violations for the 1,018 lines.

As an exhaustive search of the design space within the maximum DER capacity limits, 2,551 scenarios are evaluated with differing proportions of PV and storage from 0% to 100% of their maximum capacities, in increments of 2%. Scenarios with storage but no PV are ignored. For each scenario, PV inverters are rated with a DC-to-AC ratio of 1.2 (i.e., $S_{PV,i} = \frac{P_{PV,DC,i}}{1.2\ kWdc}\ kVA$), and the ESS inverters are rated with a 2:1 energy-to-power ratio (i.e., $S_{ESS,i} = \frac{E_i}{2\ kWh}\ kVA$). The 2,551 scenarios were run in parallel on Peregrine, the National Renewable Energy Laboratory's (NREL) high-performance computing system. Simulation parameters are given in Table 2.

Through these scenarios, trade-offs among the three key objectives – investment cost, total violations, and CPI – can be determined by sketching the Pareto front, and additional metrics can be evaluated, such as ANEI and PV curtailment (Tasks 6, 7, & 8).

Table 2. PSN Simulation Parameters

η_{RT}	η_{inv}	$\underline{SOC}$	$\overline{SOC}$	ρ	ε_Z	ε_C	ε_V
85.5%	98.4%	10%	100%	3%	10 kW	2 kW	0.005 p.u.

Multiobjective DER Scenario Analysis Results

Figures 8 to 11 show comparisons of the 2,551 DER scenarios, 10 of which did not converge in the time allotted, and highlight four scenarios, including the no-DER baseline. With PV alone, annual NZE is nominally achieved with 27.3 MW PV, shown by the ANZE-PV only scenario in Figure 8; however, when considering 15-minute NZE (Figure 9), the ANZE-PV only scenario performs poorly. CPI decreases with increasing PV capacity up to ~9 MW, at which point power backfeeding deteriorates performance (Figure 10). As expected, adding ESS to time-shift energy improves 15-minute NZE performance. For instance, the ANZE-PV+ESS scenario, with 25.8 MW of PV and 140 MWh of ESS, also achieves annual NZE but reduces CPI 76% compared to ANZE-PV only.

Together with power backfeeding, the ANZE-PV only scenario suffers from frequent operating violations (Figure 11), which the ANZE-PV+ESS scenario reduces by 89%; however, scenarios with significant violations are infeasible in practice, so it is valuable to instead determine how close the district can get to NZE without violations. In answer, the "near-0 violations" scenario is that with the lowest ANEI and CPI without significant violations. It reduces both ANEI and CPI ~78% compared to the baseline, but it incurs more than double the capital cost of the ANZE PV+ESS scenario. On the other hand, the voltage control scheme is intended to reduce but not eliminate violations; control refinement could further reduce violations once likely lower cost scenarios are selected.

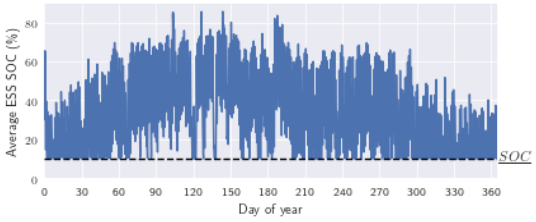

Figure 12. ANZE-PV+ESS scenario average ESS SOC, indicating the need for seasonal storage to shift summer excess PV energy to serve winter loads.

Notably, the district does not achieve zero CPI (15-minute NZE), even with extensive storage. In this analysis, ESS is operated only for intraday energy shifting. Ideally, its SOC should fluctuate from one day to the next in the mid-range without hitting its minimum or maximum limits; however, as illustrated in Figure 12 for the ANZE-PV+ESS scenario, the average ESS SOC $\left(\frac{\sum_{i\in B} SOC_i(t)}{|B|}\right)$ shows seasonal variability, reflecting the availability of ample PV generation in

summer but reduced output in winter. With only intraday shifting, ESS does not effectively address seasonal fluctuations. To avoid overbuilding PV to boost winter generation, districts with limited generation options could consider added storage for seasonal energy shifting, though applicable technologies (e.g., compressed air energy storage, pumped hydro) are more feasible for NZE cities or regions than districts. Technologies appropriate for districts (e.g., hydrogen fuel cells, flow batteries) are promising but still developing. Alternatively, the district could benefit from diversifying its generation with wind, micro-hydro, and/or biogas, if available. Other URBANopt building scenarios could also be assessed to compare more extensive DER buildouts to more advanced building measures, such as seasonal thermal storage, to bridge to gap to zero CPI.

Conclusion

This work develops an integrated building and power system model for designing districts with very high renewable energy penetrations. In this framework, impacts of both demand-side and supply-side technologies on the district's affordability, self-sufficiency, and power system reliability can be assessed. The model includes a new bilevel control scheme to manage the district's net power import and voltage rise from high distributed PV penetrations with both central and local control of DERs. The framework is applied to design the Peña Station NEXT district to illustrate the costs of achieving varying DER penetrations, up to and including annual NZE; however, the district, which has only PV generation available, is limited by seasonal fluctuations in PV output and cannot achieve NZE on a 15-minute basis, highlighting the need for seasonal electric and/or thermal storage. In future work, the modeling platform will be extended to consider other impacts on the district design, including seasonal storage, heating electrification, and electric vehicle charging. For selected scenarios, further operational optimizations can refine the voltage control and investigate the impact of forecasting errors on NZE performance. The modeling framework can be similarly applied to district retrofits and sustainable city planning to balance the various needs and goals of the stakeholders, including the municipality, customers, land developer, and utility.

Subject Inventions Listing:

None

ROI #:

None

Responsible Technical Contact at Alliance/NREL:

Bri-Mathias Hodge | Bri.Mathias.Hodge@nrel.gov

Name and Email Address of POC at Company:

Peter Jacobson (Panasonic) | Peter.Jacobson@us.panasonic.com

DOE Program Office:

Office of Energy Efficiency and Renewable Energy, Grid Integration Program